Forming and implementing a hyperchaotic system with rich dynamics

Liu Wen-Bo(刘文波)[a)†], Wallace K. S. Tang(邓樑生)[b)], and Chen Guan-Rong(陈关荣)[b)]

[a)] *College of Automatic Engineering, Nanjing University of Aeronautics and Astronautics, Nanjing* 210016, *China*
[b)] *Department of Electronic Engineering, City University of Hong Kong, Kowloon, Hong Kong SAR, China*

(Received 27 September 2010; revised manuscript received 30 May 2011)

A simple three-dimensional (3D) autonomous chaotic system is extended to four-dimensions so as to generate richer nonlinear dynamics. The new system not only inherits the dynamical characteristics of its parental 3D system but also exhibits many new and complex dynamics, including assembled 1-scroll, 2-scroll and 4-scroll attractors, as well as hyperchaotic attractors, by simply tuning a single system parameter. Lyapunov exponents and bifurcation diagrams are obtained via numerical simulations to further justify the existences of chaos and hyperchaos. Finally, an electronic circuit is constructed to implement the system, with experimental and simulation results presented and compared for demonstration and verification.

Keywords: chaotic circuit, circuit implementation, hyperchaotic system, Lyapunov exponent

PACS: 05.45.Jn **DOI:** 10.1088/1674-1056/20/9/090510

1. Introduction

In the last few years, the generation of hyperchaos has provoked a lot of interest from the nonlinear science community. Several new hyperchaotic systems have been found or constructed,[1−11] which has boosted research on hyperchaos control[12,13] and the application of hyperchaos in multi-frequency oscillatory signal generation, fluid dynamics and data encryption.[14,15]

Many hyperchaotic systems are obtained by extending a three-dimensional (3D) chaotic system, such as the Lorenz,[16] Chen[17] and Lü[18,19] systems, or the other simple quadratic chaotic systems,[20] to four or even higher dimensions. It was reported that hyperchaos can be observed via applying an external sinusoidal excitation to a chaotic system.[4] Another possible approach is to introduce an additional system state, through a linear or nonlinear dynamical equation.[2]

Inspired by the above-mentioned findings and designs, in this paper, a new hyperchaotic system is constructed based on the 3D autonomous chaotic system proposed in Ref. [21]. Compared with other hyperchaotic systems similarly designed and constructed, this new hyperchaotic system possesses much richer dynamics, exhibiting 1-scroll, 2-scroll and 4-scroll chaotic attractors, and a hyperchaotic attractor.

The organization of the paper is as follows. In Section 2, the formation of the new hyperchaotic system is described and some basic analyses are presented. To verify the existence of the observed chaotic and hyperchaotic attractors, the Lyapunov exponent spectrum and the associated bifurcation diagrams are computed and demonstrated in Section 3. In Section 5, an electronic circuitry is designed and implemented, with both simulated and experimental results presented for comparison. Finally, a brief conclusion is drawn in Section 6.

2. Formation of the hyperchaotic system

Since the generation of a double-scroll attractor from the chaotic Chua circuit,[22] tremendous interest has been provoked in the generation multi-scroll attractors. In Ref. [21], a 3D autonomous chaotic system was proposed,

$$\begin{aligned} \dot{x}_1 &= ax_1 - x_2x_3, \\ \dot{x}_2 &= -bx_2 + x_1x_3, \\ \dot{x}_3 &= -cx_3 + x_1x_2, \end{aligned} \tag{1}$$

where $b > c > 0$ and $b + c > a > 0$. A double 2-scroll chaotic attractor exists in, and can be observed from, this system.[23,24]

†Corresponding author. E-mail: wenboliu@nuaa.edu.cn

© 2011 Chinese Physical Society and IOP Publishing Ltd

Here, we will generate chaotic and hyperchaotic attractors by slightly modifying Eq. (1) to obtain rich and complex dynamics. Assuming that a new system state x_4 is coupled to the state equation of x_2, the following 4D nonlinear system is constructed:

$$\begin{aligned}\dot{x}_1 &= ax_1 - x_2x_3,\\ \dot{x}_2 &= -bx_2 + x_1x_3 + ex_4,\\ \dot{x}_3 &= -cx_3 + x_1x_2,\\ \dot{x}_4 &= dx_4 + fx_1x_3,\end{aligned} \tag{2}$$

where constants $e > 0$, and d and f are to be determined.

Based on the bifurcation analysis and computer simulations, to be detailed in Section 3 below, system (2) can indeed generate very rich chaotic and hyperchaotic dynamics when d and f are of the same sign. To simplify the circuitry implementation later on, let $f = -1$ in Eq. (2), we obtain

$$\begin{aligned}\dot{x}_1 &= ax_1 - x_2x_3,\\ \dot{x}_2 &= -bx_2 + x_1x_3 + ex_4,\\ \dot{x}_3 &= -cx_3 + x_1x_2,\\ \dot{x}_4 &= -dx_4 - x_1x_3,\end{aligned} \tag{3}$$

where a, b, c, d and e are positive constants with $b + c > a$.

2.1. Symmetry and invariance

From Eq. (3), we know that the system is symmetric with coordinate transformations

$$\begin{aligned}&(x_1, x_2, x_3, x_4) \to (x_1, -x_2, -x_3, -x_4),\\ &(x_1, x_2, x_3, x_4) \to (-x_1, -x_2, x_3, -x_4),\\ &(x_1, x_2, x_3, x_4) \to (-x_1, x_2, -x_3, x_4).\end{aligned}$$

Therefore, the system is symmetric about the coordinate planes x_1–x_3 and x_2–x_4. It is easy to verify that all the axes are solution orbits, while the one along the x_1-axis tends to infinity but the others tend to the origin as $t \to \infty$.

2.2. Equilibria and stability

The equilibria of (3) can be easily found by letting $\dot{x}_1 = \dot{x}_2 = \dot{x}_3 = \dot{x}_4 = 0$, yielding

$$\begin{aligned}&ax_1 - x_2x_3 = 0, \quad -bx_2 + x_1x_3 + ex_4 = 0,\\ &-cx_3 + x_1x_2 = 0, \quad -dx_4 - x_1x_3 = 0.\end{aligned}$$

In the case of $e < d$, there are five real equilibria, given by

$$\begin{aligned}&E_0 = (0, 0, 0, 0), \quad E_1 = (x_{1+}, x_{2+}, x_{3+}, x_{4-}),\\ &E_2 = (x_{1+}, x_{2-}, x_{3-}, x_4),\\ &E_3 = (x_{1-}, x_{2+}, x_{3-}, x_{4-}),\\ &E_4 = (x_{1-}, x_{2-}, x_{3+}, x_{4+}),\end{aligned}$$

where $x_{1\pm} = \pm\sqrt{bcd/(d-e)}$, $x_{2\pm} = \pm\sqrt{ac}$, $x_{3\pm} = \pm\sqrt{abd/(d-e)}$, and $x_{4\pm} = \pm\frac{b}{d-e}\sqrt{ac}$.

Note that these equilibria have some kinds of symmetry with respect to the origin or the coordinate planes, attributing to the symmetry property of the system (3). This is quite similar to the case with system (1), which has five real equilibria, namely $\hat{E}_0 = (0, 0, 0)$, $\hat{E}_1 = (x_{1+}, x_{2+}, x_{3+})$, $\hat{E}_2 = (x_{1+}, x_{2-}, x_{3-})$, $\hat{E}_3 = (x_{1-}, x_{2+}, x_{3-})$, $\hat{E}_4 = (x_{1-}, x_{2-}, x_{3+})$ with $x_{1\pm} = \pm\sqrt{bc}$, $x_{2\pm} = \pm\sqrt{ac}$, $x_{3\pm} = \pm\sqrt{ab}$. However, if $e \geq d$, then there is only one real equilibrium, E_0, and the dynamics of system (3) will behave much differently from the original system (1), as further illustrated in Section 4.2 below.

The Jacobian matrix of Eq. (3) is

$$\boldsymbol{J} = \begin{bmatrix} a & -x_3 & -x_2 & 0\\ x_3 & -b & x_1 & e\\ x_2 & x_1 & -c & 0\\ -x_3 & 0 & -x_1 & -d \end{bmatrix}. \tag{4}$$

The eigenvalues of (4) evaluated at E_0 are found to be $\lambda_1 = a$, $\lambda_2 = -b$, $\lambda_3 = -c$, and $\lambda_4 = -d$. Since a, b, c, d are positive, one has $\lambda_1 > 0$, λ_2, λ_3, $\lambda_4 < 0$ and hence E_0 (the origin) is a saddle point in the 4D phase space with instability index of one.

Similarly, one can obtain the eigenvalues of Eq. (4) at other equilibria. By linearizing system (3) about the other four equilibria, the following characteristic equation is obtained:

$$f(\lambda) = \lambda^4 + A\lambda^3 + B\lambda^2 + C\lambda + D, \tag{5}$$

where $A = (b + c + d - a)$, $B = dc + bd - ad + be\,(a - c)/(d - e)$, $C = 4abcd/(d - e)$, and $D = 4abcd$.

Assuming that λ_1, λ_2, λ_3 and λ_4 are the eigenvalues obtained by solving Eq. (5), we can conclude

1) Since $d > a - b - c > 0$, one has $A > 0$, so the sum $S_\lambda = \lambda_1 + \lambda_2 + \lambda_3 + \lambda_4 < 0$.

2) Since a, b, c, $d > 0$, one has $D > 0$, so the real parts of the eigenvalues are either all negative (the case with all positive eigenvalues is impossible because $S_\lambda < 0$) or two of them are positive while the other two are negative.

In order to further analyse the stability of these equilibria, numerical simulations are carried out for some fixed parameters with $d > e$. A typical example is depicted in Fig. 1. It is found that Eq. (5) has

two negative real eigenvalues, $\lambda_3 < 0$ and $\lambda_4 < 0$, together with a pair of complex conjugate eigenvalues, $\lambda_{1,2} = \sigma \pm \mathrm{j}\, w$, where $\sigma > 0$ in the case of chaos. These four equilibria are all unstable with an instability index of two, having similar features to the original 3D system (1), which was discussed in Refs. [23] and [24]. Based on this numerical analysis, it is concluded that the five equilibria of system (3) are all unstable if $d > e$.

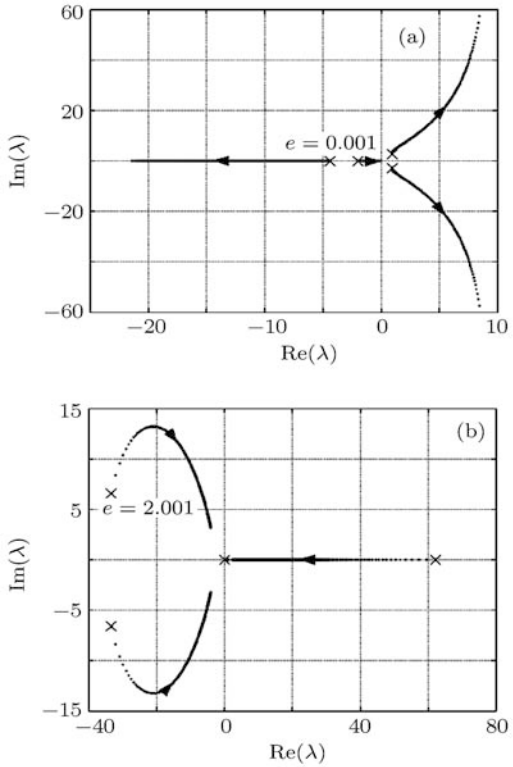


Fig. 1. Eigenvalues of system (3) at non-origin equilibria: $a = 2$, $b = 3$, $c = 1.5$, $d = 2$. (a) e is varied from 0.001 to 1.9; (b) e is varied from 2.001 to 3.0.

3. Bifurcation diagrams and Lyapunov exponents

In this section, the complex dynamics of system (3) are further investigated by combining bifurcation analysis and numerical simulations. Fix $a = 2$, $b = 3$, $c = 1.5$, $d = 2$ and let e be varied from 0.001 to 3, results in Figs. 2 (a) and 2 (b) are obtained, showing the spectrum of the system Lyapunov exponents and the corresponding bifurcation diagram of state x_3 with respect to e. It can be observed that, as e increases, the dynamics of system (3) undergoes the following routes:

1) When $0 < e < 0.49$, the system is periodic.

2) When $0.49 < e < 2.55$, the system is chaotic. However, it is also noticed that many different kinds of chaotic attractors can be obtained. There also exist many periodic orbits and quasiperiodic orbits in the same parameter ranges, which will be further detailed in Section 4.1 and Section 4.2.

3) When $2.55 < e < 3$, the system is mainly in its hyperchaotic state and the Lyapunov dimension is larger than 3. At the same time, many periodic windows emerge (some state-space diagrams of the hyperchaotic attractors will be presented in Section 4.3). It should be remarked that within this range of e, one has $d < e$ and system (3) only has one zero equilibrium.

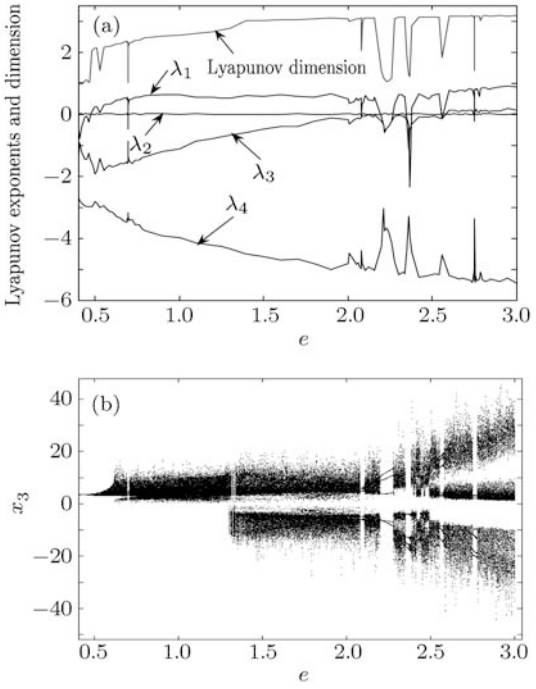


Fig. 2. (a) Lyapunov exponents versus e, (b) bifurcation diagram of system (3), with $a = 2$, $b = 3$, $c = 1.5$, $d = 2$ and $e \in [0.4, 3]$.

4. State space diagrams

To visualize the state trajectories of the system, simulations have been carried out for some typical parametric values, revealing very rich complex dynamics.

4.1. Periodic states

Referring to Fig. 2(b), we can find many periodic windows in-between the chaotic and hyperchaotic states. Figure 3 shows some typical periodic phase portraits in the x_1–x_3 plane.

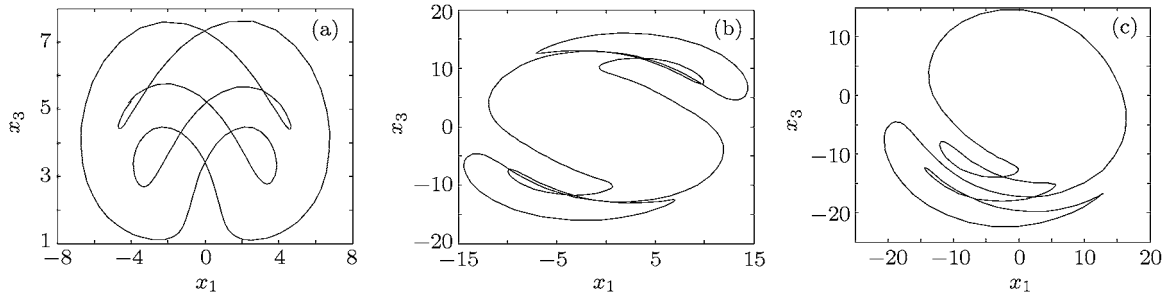


Fig. 3. Phase portraits of periodic trajectories in the x_1–x_3 plane, with $a = 2$, $b = 3$, $c = 1.5$, $d = 2$, and $e = 0.697$, 2.25 or 2.36, respectively. (a) $e = 0.697$, (b) $e = 2.25$, (c) $e = 2.36$.

4.2. Chaotic states

Different kinds of chaotic attractors can be obtained from system (3). In order to distinguish their structures, the attractors are defined as 4-scroll, 2-scroll and 1-scroll (or 4-wings, 2-wings and 1-wing) according to their shapes in the x_1–x_3 (x_2–x_3) plane.

4.2.1. The 4-scroll chaotic attractors

According to the bifurcation diagram shown in Fig. 2(b), the trajectories of state $x_3(t)$ pass through both regions of $x_3(t) > 0$ and $x_3(t) < 0$, forming a 4-scroll attractor in the x_1–x_3 plane (or a 4-wing attractor in the x_2–x_3 plane), as shown in Fig. 4.

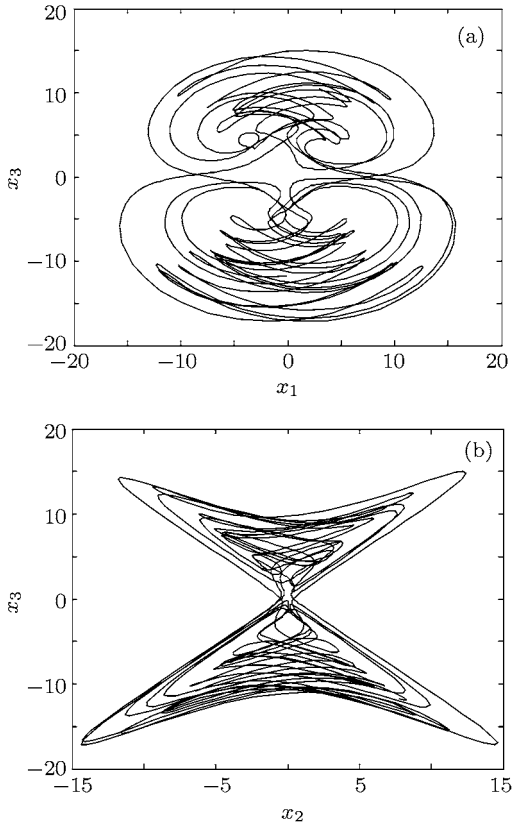


Fig. 4. The 4-scroll attractor with $a = 2$, $b = 3$, $c = 1.5$, $d = 2$, $e = 1.6$. (a) x_1–x_3 plane; (b) x_2–x_3 plane.

4.2.2. The 2-scroll chaotic attractors

When $e < 1.3$, the trajectories are limited in the regions of $x_3(t) > 0$ or $x_3(t) < 0$. Therefore, only an upper attractor ($x_3(t) > 0$) or a lower attractor ($x_3(t) < 0$) appears. For example, when $e = 1.0$, the trajectory forms a 2-scroll attractor in the x_1–x_3 plane (or a 2-wing attractor in the x_2–x_3 plane), as shown in Fig. 5. This kind of chaotic attractor is called a 2-scroll upper attractor (the 2-scroll lower attractor is similarly defined). The trajectories of these 2-scroll attractors run around the two equilibria, E_1 and E_4 or E_2 and E_3, depending on its location.

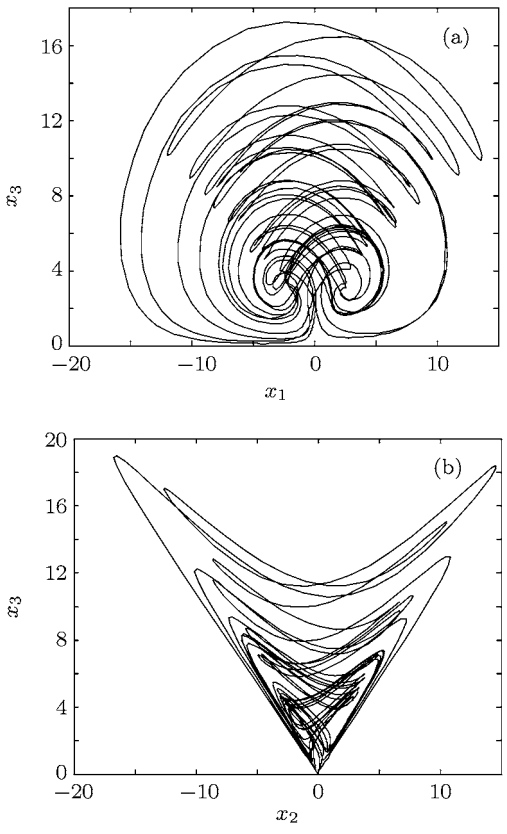


Fig. 5. The 2-scroll attractor with $a = 2$, $b = 3$, $c = 1.5$, $d = 2$, $e = 1.0$. (a) x_1–x_3 plane; (b) x_2–x_3 plane.

The other two kinds of 2-scroll attractors, denoted as the left-sided and right-sided 2-scroll attractors, respectively, can also be observed. The trajectories run around the two equilibria, E_3 and E_4 or E_1 and E_2, for example a right-sided 2-scroll attractor (around the equilibria E_3 and E_4), are shown in Fig. 6.

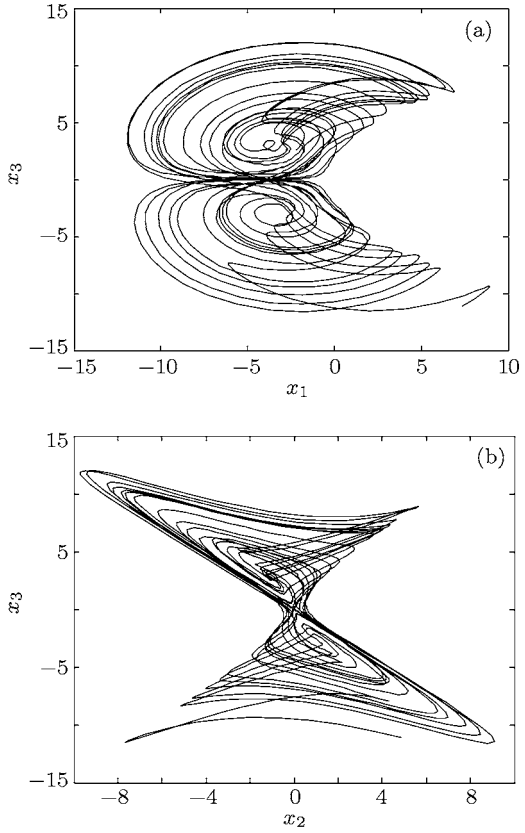


Fig. 6. The two-scroll with $a = 1$, $b = 3$, $c = 1.5$, $d = 2$, $e = 1.6$. (a) x_1–x_3 plane, (b) x_2–x_3 plane.

4.2.3. Single-scroll attractors

When the chaotic trajectory runs around only one equilibrium (any one from E_1 to E_4), a single-scroll attractor can be observed, as shown in Fig. 7.

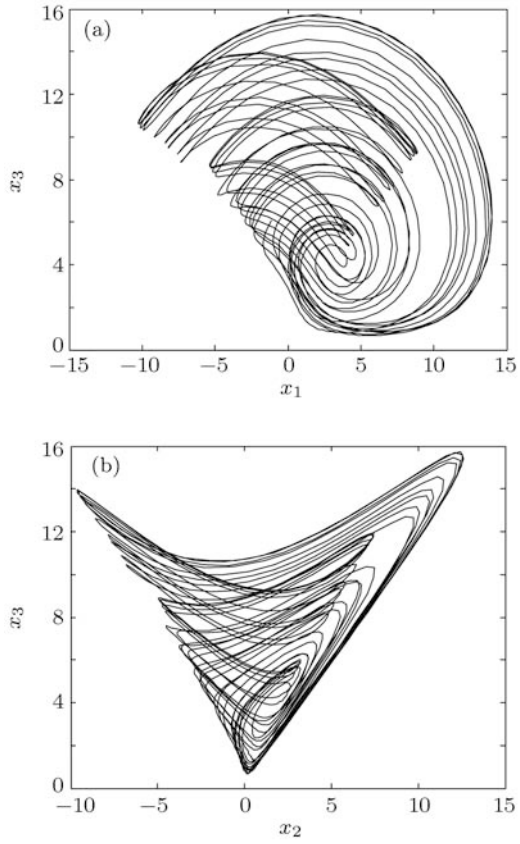


Fig. 7. Single scroll attractor with $a = 2.3$, $b = 3$, $c = 1.5$, $d = 2.5$, $e = 1.8$. (a) x_1–x_3 plane, (b) x_2–x_3 plane.

4.3. Hyperchaotic states

Hyperchaos emerges when $e > d$, even if there exists only one equilibrium. As shown in Figs. 8 and 9, the topological properties of the hyperchaotic attractors are largely different from the chaotic attractors reported above.

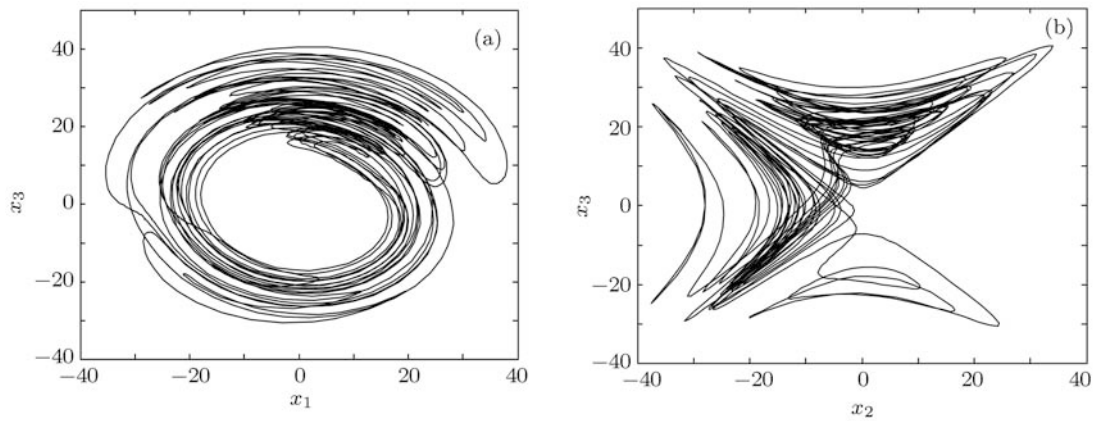


Fig. 8. Hyperchaotic attractor with $a = 2$, $b = 3$, $c = 1.5$, $d = 2$, $e = 2.74$ (The computed Lyapunov exponents are: 0.793, 0.201, 0.000, −5.387). (a) x_1–x_3 plane, (b) x_2–x_3 plane.

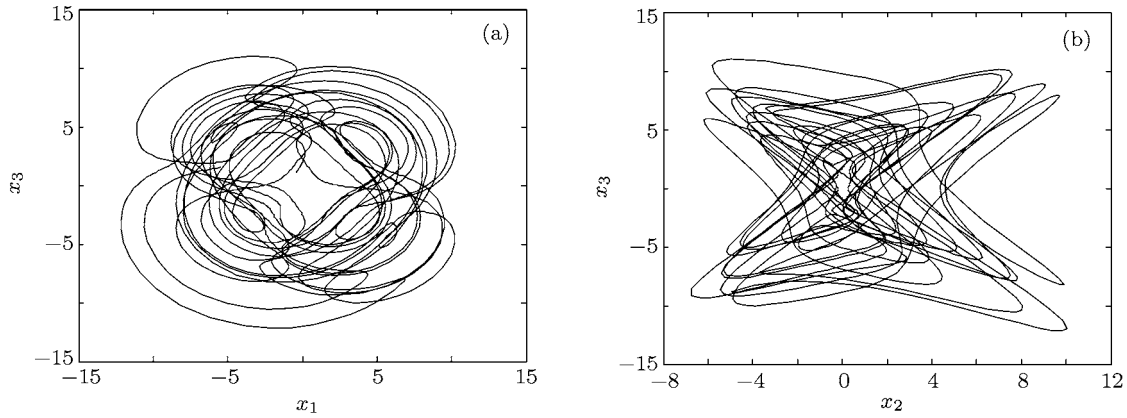


Fig. 9. Hyperchaos attractor with $a = 1$, $b = 3$, $c = 1.5$, $d = 2$, $e = 2.7$ (The computed Lyapunov exponents are: 0.812, 0.213, 0.000, −5.461). (a) x_1–x_3 plane, (b) x_2–x_3 plane.

5. Circuitry design and implementation

The new system described by Eq. (3) has been realized with an electronic circuit, as shown in Fig. 10, where the operational amplifiers and associated circuitry perform the basic operations of addition, subtraction and integration. The nonlinear terms in the state equations are implemented via performing multiplications by the analog multipliers AD633.

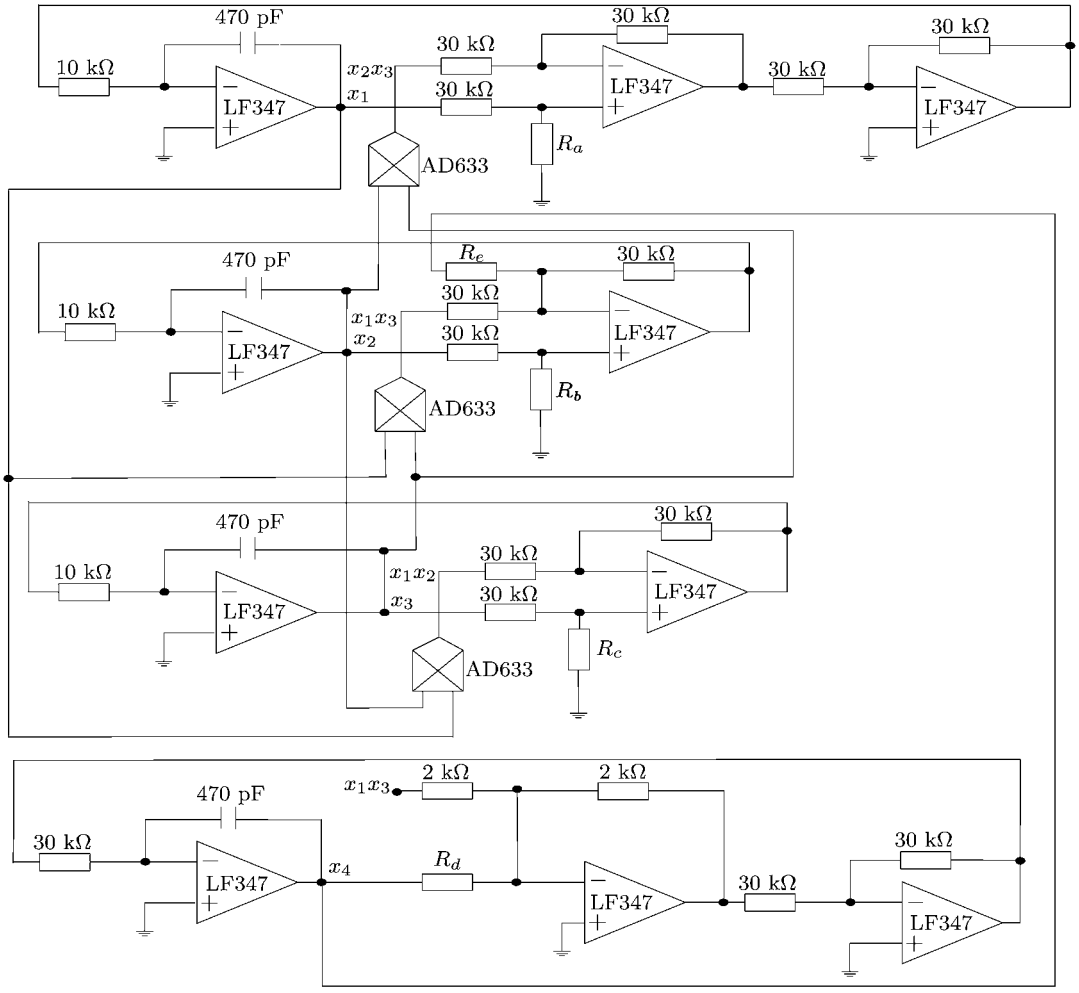


Fig. 10. Circuit realization of system (3).

The bifurcation process and various dynamics of system (3) can be obtained by simply tuning the resistances of R_a, R_b, R_c, R_d and R_e in Fig. 10, which correspond to the system parameters a, b, c, d and e in Eq. (3), respectively.

Figure 11 depicts two periodic orbits of system (3) with different sets of parameters. Assume that $R_a = 1$ kΩ, $R_b = 3$ kΩ, $R_c = 2$ kΩ, $R_e = 50$ kΩ are fixed and R_d is varied. We obtain different types of chaotic or hyperchaotic attractors, as shown in Fig. 12. By comparison, a good qualitative agreement between the numerical simulation and the experimental realization is confirmed.

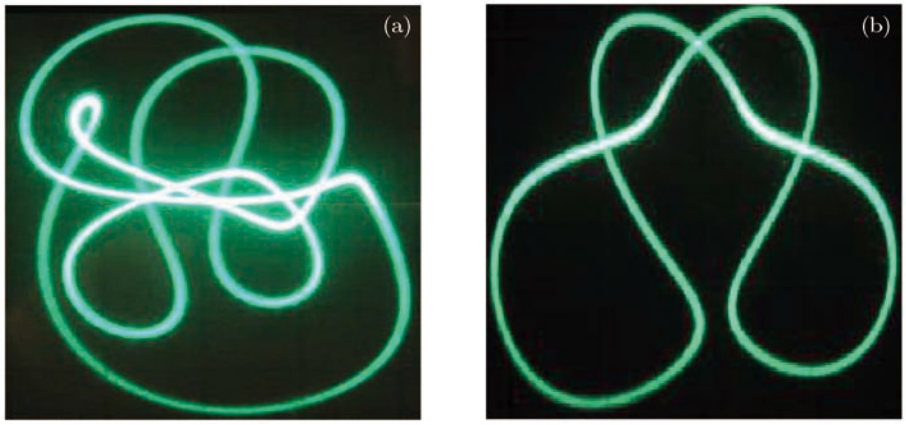


Fig. 11. (colour online) Phase portraits of periodic orbits obtained from the system (3) in the x_1–x_3 plane: (a) $R_a = 185$ Ω, $R_b = 10.77$ kΩ, $R_c = 2.73$ kΩ, $R_d = 6.4$ kΩ and $R_e = 113$ kΩ; (b) $R_a = 1$ kΩ, $R_b = 3$ kΩ, $R_c = 2$ kΩ, $R_d = 5.7$ kΩ and $R_e = 50$ kΩ.

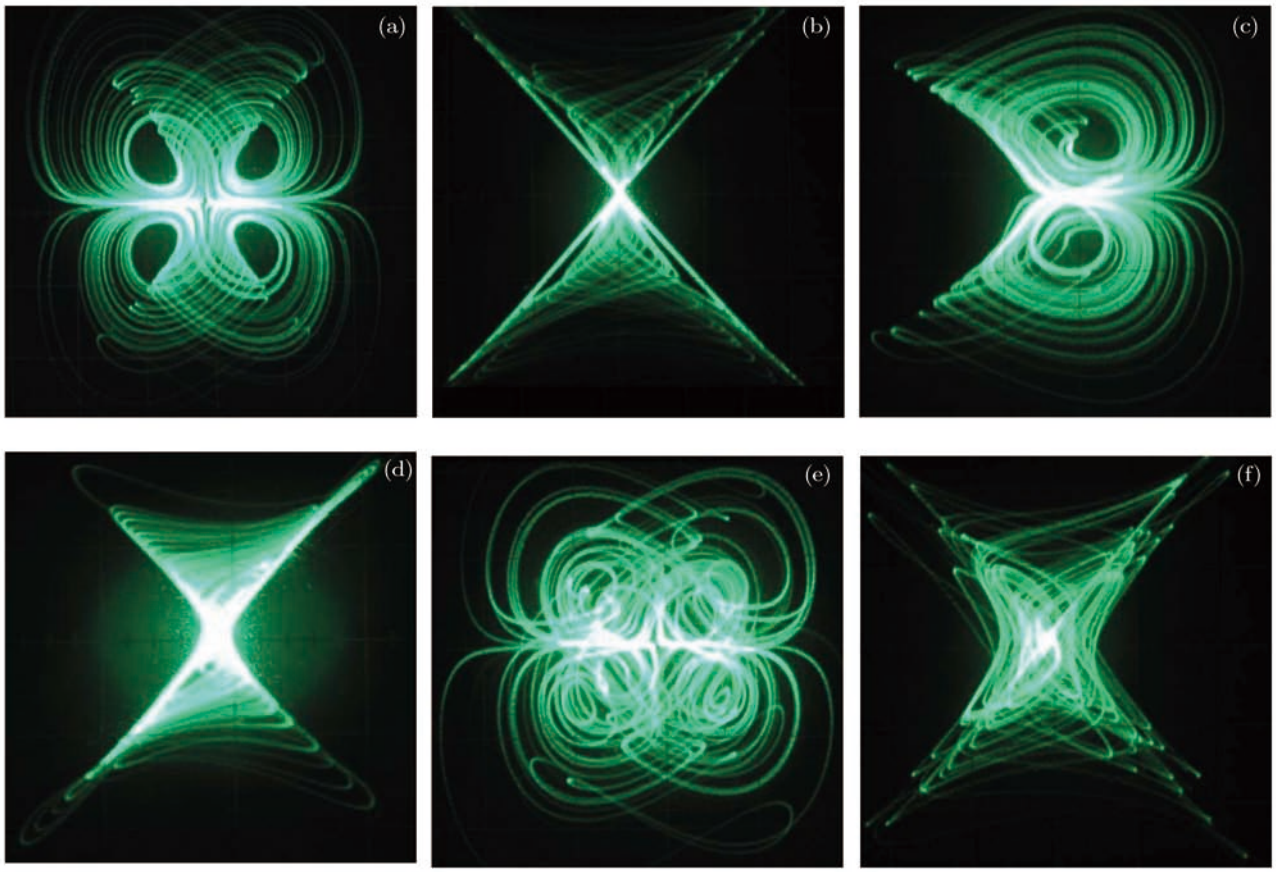


Fig. 12. (colour online) 4-scroll attractor in (a) the x_1–x_3 plane; (b) the x_2–x_3 plane, when $R_d = 1.86$ kΩ; 2-scroll attractor in (c) the x_1–x_3 plane; (d) the x_2–x_3 plane, when $R_d = 3.19$ kΩ; hyperchaotic attractor in (e) the x_1–x_3 plane; (f) the x_2–x_3 plane, when $R_d = 5.7$ kΩ.

6. Conclusion

This paper reports the formation of a 4D nonlinear system by extending a previously designed 3D chaotic system via the addition of a simple term while keeping the original symmetry. Thereby, the new system is able to generate very rich nonlinear dynamics including different kinds of chaotic and hyperchaotic attractors, confirmed by the Lyapunov exponent spectrum and bifurcation diagrams. A physical circuit is built and experimented, verifying all the numerical observations. It is believed that coordinate symmetry plays an important role in such complex dynamics, while the other parts of the system can be extremely simple, which is an interesting topic to be further explored.

References

[1] Hu G 2009 *Int. J. Bifur. Chaos* **19** 651

[2] Li Y X, Tang K S and Chen G R 2005 *Int. J. Bifur. Chaos* **15** 3367

[3] Li Y X, Tang K S, Chen G R and Su X 2007 *Dynamics of Continuous, Discrete and Impulsive Systems Series* B: *Applications & Algorithms* **14** 97

[4] Li Y X, Chen G R and Tang K S 2005 *IEEE Trans. Cir. Syst.*-II **52** 204

[5] Liu M H, Feng J C and Tse C K 2010 *Int. J. Bifur. Chaos* **20** 1201

[6] Mahmoud G M, Mahmoud E E and Ahmed M E 2009 *Nonlinear Dynam.* **58** 725

[7] Musielak Z E and Musielak D E 2009 *Int. J. Bifur. Chaos* **19** 2823

[8] Wang G Y, Zhang X, Zheng Y and Li Y X 2006 *Physica* A **371** 260

[9] Wang G Y, Zheng Y and Liu J B 2007 *Acta Phys. Sin.* **56** 3113 (in Chinese)

[10] Wang X Y and Chao G B 2010 *Int. J. Mod. Phys.* B **24** 4619

[11] Yang Q G, Zhang K M and Chen G R 2009 *Nonlinear Anal. — Real World Applications* **10** 1601

[12] Huang L L, Xin F and Wang L Y 2011 *Acta Phys. Sin.* **60** 010505 (in Chinese)

[13] Feng X Q, Yao Z H, Tian Z L and Han X Y 2010 *Acta Phys. Sin.* **59** 8414 (in Chinese)

[14] Wang J and Jiang G P 2011 *Acta Phys. Sin.* **60** 060503 (in Chinese)

[15] Min F H and Wang E R 2010 *Acta Phys. Sin.* **59** 7657 (in Chinese)

[16] Lorenz E N 1963 *J. Atmos. Sci.* **20** 130

[17] Chen G R and Ueta T 1999 *Int. J. Bifur. Chaos* **9** 1465

[18] Lü J and Chen G R 2002 *Int. J. Bifur. Chaos* **12** 659

[19] Lü J, Chen G R, Cheng D and Celikovský S 2002 *Int. J. Bifur. Chaos* **12** 2917

[20] Yang Q G and Chen G R 2008 *Int. J. Bifur. Chaos* **18** 1393

[21] Liu W B and Chen G R 2003 *Int. J. Bifur. Chaos* **13** 261

[22] Chua L O, Matsumoto T and Komuro M 1985 *IEEE Trans. Cir. Syst.* **32** 798

[23] Liu W B and Chen G R 2004 *Int. J. Bifur. Chaos* **14** 971

[24] Liu W B and Chen G R 2004 *Int. J. Bifu. Chaos* **14** 1395